Glued Laminated Timber from Oil Palm Timber – Beam Structure, Production and Elastomechanical Properties

Lena Heister and Katja Fruehwald-Koenig

Abstract Oil palm timber used for load-bearing purposes such as glued laminated timber (GLT) needs to have clearly defined strength and stiffness values. Because the wood density (which correlates to elastomechanical properties) varies significantly within oil palm trunks, oil palm boards must be graded based on their density across the board width in order to homogenize and improve the properties of the final product. In this preliminary investigation, 20 beams of combined GLT with four different types of graded lamellas were produced and tested in a 4-point-bending test. The results show a correlation between density and bending strength. The characteristic strength values are achieved, and the elastomechanical properties of beams based on lamellas that are ripped lengthwise and edge-glued according to their density are higher compared to beams based on lamellas cut only according to their geometry. A correlation between bending strength and local MOE is determined. In summary, lengthwise ripping of oil palm boards according to their density across the board width as well as a grading according to density limit values is shown to improve the properties of combined GLT made from oil palm timber for load-bearing purposes.

Keywords GLT · Oil palm timber · Density · GLT production · Properties · Building products

1 Introduction

Oil palm trees (*Elaeis guineensis* JACQ.) are mainly cultivated in large plantations for palm oil production and used for food, chemicals, pharmaceuticals and bioenergy. The palm trees' oil productivity decreases after 20 years of age. Therefore, plantations are renewed every 25–30 years. Each year a large supply of oil palm trunks (some 200 million m^3 per year worldwide, with over 80% in Southeast Asia) is traditionally considered as waste. Recent research, however, has explored the potential

L. Heister · K. Fruehwald-Koenig (✉)
Departement of Production Engineering and Wood Technology, Ostwestfalen-Lippe University of Applied Sciences and Arts, Lemgo, Germany
e-mail: katja.fruehwald@th-owl.de

M. Jawaid et al. (eds.), *Proceedings of 2nd World Conference on Byproducts of Palms and Their Applications*, Springer Proceedings in Materials 19,
https://doi.org/10.1007/978-981-19-6195-3_3

commercial uses of oil palm wood [1]. In many cases the wood can substitute for tropical hardwoods, e.g. used as panels (blockboards, flash doors, multi-layer solid wood panels) and softwoods in construction timber (GLT, CLT). Only few studies were made on building products: [2] tested rafters with small binders and [3] tested the compression properties of oil palm wood CLT. Numerous studies show that the elastomechanical properties of oil palm wood vary with the density along the height and diameter of oil palm trunks [4–11]. Therefore, conventional sawing patterns lead to density and further strength and stiffness gradients within the cross-section of boards. In order to use oil palm timber for load-bearing products with defined elastomechanical properties, strength grading must be carried out. [12] showed that existing X-ray devices, if properly calibrated, can be used for oil palm lumber. The aim of this preliminary investigation is to determine elastomechanical properties of GLT made from strength graded oil palm wood. Therefore, 20 beams of combined GLT from oil palm wood with four different types of strength graded lamellas were produced and tested in a 4-point-bending test. These initial tests intend to show that, firstly, grading according to density limit values and the specific arrangement of the lamella within the glulam beam and, secondly, lengthwise ripping of oil palm boards according to their density across the board width both lead to an improvement of the elastomechanical properties of GLT made from oil palm lumber for load-bearing purposes.

2 Material and Methods

2.1 Oil Palm Wood Material

The material was taken from 30-year-old oil palms (*Elaeis guineensis* JACQ.) grown near Kluang/Johor, Malaysia. In 2016, a total of 150 palms were harvested for sawmilling and drying studies by PalmwoodNet and the Forest Research Institute of Malaysia (FRIM). The sawing pattern is shown in Fig. 1. The denser material in the periphery was cut to 30 mm (fresh) and had a thickness after kiln drying of 27 mm, the lower dense material from the centre was cut into 55 mm (fresh) resp. 50 mm (kiln-dried) boards. The kiln-dried material was shipped to Germany. For the production of GLT, 70 boards of 27 mm thickness from 20 different logs and two different trunk heights were taken. The lower trunk section was from 1–4 m and the middle trunk section from 4–7 m trunk height above ground. The mean length of the boards was 2.8 m and width 0.22 m.

Due to the anatomical structure of monocotyledons, it was assumed that opposite boards have comparable elastomechanical properties. For the pairwise comparison in this investigation, two outer and two inner 27 mm boards placed opposite to each other were selected by visual inspection. Boards with cracks or cell collapse were not used. The edges of the boards were trimmed along the cortex using a table saw. Due to the natural taper of the oil palm trunks (some 0.8 cm per meter trunk length),

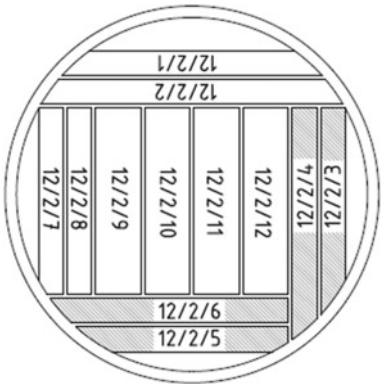

Fig. 1 Sawing pattern of the oil palm trunk sections with board identification numbers

the boards had different widths at each end (approx. 2–3 cm difference). The rough-cut lamellas were calibrated using a two-side planer with HeliPlan tools from Leitz, Germany, one board of each pair to a thickness of 20 mm, the other to 17 mm.

2.2 Calculation of Lamella Strength Class Limits

Because there is no existing grading standard for oil palm wood and the small dimensions of the GLT produced within this investigation, the strength grading of the oil palm lumber was based on the European strength class system for coniferous lumber (C-classes) according to [13, 14]. The statistic calculation model of [14], attachment B was used in modified form (Eq. 1) to calculate the density limits for the strength classes, based on the relationship between density as indicating property (IP) and tensile strength ($f_{t,0} = 1E\text{-}05\rho^{2.38}$) resp. compression strength ($f_{c,0} = 2E\text{-}05\rho^{2.24}$) parallel to the vascular bundles for MOR determined in preliminary investigations on small test specimens, published in [11] and linearized by the natural logarithm. The 5% probability level and therefore $t = 1.645$ was assumed.

$$\begin{aligned} MOR &= a_{MOR} IP + b_{MOR} - t \cdot s_{\delta,MOR} \\ \rightarrow IP &= \frac{MOR - b_{MOR} + t \cdot s_{\delta,MOR}}{a_{MOR}} \end{aligned} \tag{1}$$

For strength class C14 [13], the characteristic tensile strength value parallel to the fibers ($f_{t,0,k} = 7.2$ MPa) leads to a density limit value of 427 kg/m^3 and the characteristic compression strength ($f_{c,0,k} = 16$ MPa) to a density range of 363–427 kg/m^3. Because of the high share of oil palm wood material with densities below 350 kg/m^3, property values for an assumed strength class C10 were extrapolated with 290–335 kg/m^3 for the compression lamellas and 335–363 kg/m^3 for the tension lamellas.

The density limit value for the shear lamellas in the middle was <290 kg/m^3 for both beam setups.

2.3 Strength Grading of the Boards

When grading boards according to their density, the average density of the board must not be assumed because the density gradient over the trunk's cross-section is higher compared to the gradient along the trunk height [15]. Figure 2 shows the density profile across the 140 mm width of a board from the outer area of the trunk.

The 17 mm thick board of each pair was used to "conventional" cut the boards according to their geometry in two 55 mm wide and 2200 mm long lamellas from each side of the board, which resulted in "full size" cross-section (= non-ripped) lamellas (Fig. 2, left). This resulted in lamellas with a density gradient over the cross-section from approximately 800–350 kg/m^3. The mean density of each non-ripped lamella was determined according to DIN 52182 [16].

The 20 mm thick board of each pair was density measured over the board width using X-ray. Therefore, 5 cm long specimens were cut from both ends of the boards, the thickness of the specimens was given by the board thickness. The specimens were planed, rectangular cut and conditioned at a standard climate of 20 °C/65% rh [17]. The X-ray measurements were performed using DENSE-LAB X from Electronic Wood Systems (EWS), Hameln. The specimens were aligned in the holding device in a way that allowed the X-ray beam to travel through the specimen at the middle of the specimen thickness. The specimen holder moved with a constant measuring speed

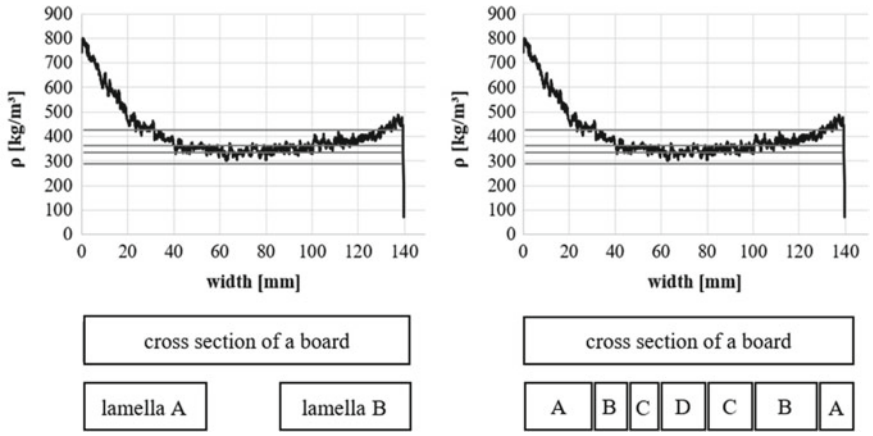

Fig. 2 Density profile of a board from the outer area of an oil palm trunk with a high density gradient over the board width. Cutting of "full size" lamellas according to their geometry with inhomogeneous density (left) and cutting strips with individual width and homogeneous density (right)

of 0.83 mm/s, measurements were taken at every 0.1 mm of the specimen. Based on the measured density profile from the end with the lower density (according to [15], it is assumed that this is the upper end), the cutting positions of each board were calculated from the smoothed density profile with a specially developed software. The minimum strip width is 10 mm. Figure 3 shows an example of a density profile with a smoothed and respectively non-smoothed curve and the calculation of the cutting positions (vertical grey wide columns). The boards were ripped lengthwise from the upper end to strips with individual width (Fig. 2, right). The grade assigned to each strip was verified by determining the mean density of each strip from mass and volume. Due to the longitudinal density distribution, the density is higher at the lower end of the board. This leads to a deviation between the calculated X-ray density class and the measured mean density of the strip. Each strip was marked with the grading class and individual strip number for further traceability. The strips were grouped according to their grade and randomly within the grading class edge-glued into timber boards (Fig. 4). Two to six strips were required to achieve the glued timber board width of 175 mm. A fibre-reinforced, one-component polyurethane adhesive (Jowapur® 686.60) was used for the edge-gluing. After curing and conditioning, the edge-glued timber boards were calibrated to the final thickness of 17 mm (Fig. 4). Three ripped lamellas were cut in width (55 mm) and length (2200 mm) from each edge-glued board. After lamella preparation, the average density was measured in laboratory conditions according to DIN 52182 [16]. Ultimately, the ripped lamellas showed a more uniform density over their width compared to the non-ripped lamellas.

2.4 Production of Glued Laminated Timber (GLT)

Six strength-graded lamellas were arranged within the combined GLT beam according to Fig. 5. Due to the low number of ripped and non-ripped lamellas of grading class <290 kg/m^3, additional non-ripped lamellas were produced from the low density boards from the center of the same trunk sections. The boards were processed in accordance with the manufacturing steps of the non-ripped lamellas described in Sect. 2.3.

The same resin was used for gluing the GLT as for the edge-gluing (Jowapur® 686.60), the mean adhesive application rate was approx. 350 g/m^2. Pressing of the GLT was done at MINDA Industrieanlagen in Minden, Germany on a modified press, TimberPress X 300 (Fig. 6, left), commonly used to produce CLT. The dimensions of the TimberPress X are 3.4 m in length and 1.2 m in width. The press has two lengthwise divided pressing plates (Fig. 6, right), each 0.6 m wide, which can be individually controlled by a hydraulic pressure system. The beams were pressed with the specific pressure of 0.75 MPa for a minimum of 240 min. After storing the beams in a standard climate [17], the beams were calibrated to the final width of 50 mm and stored again in the standardized climate until testing. In summary, 20 beams with different beam setups and from different lamella strength classes were produced.

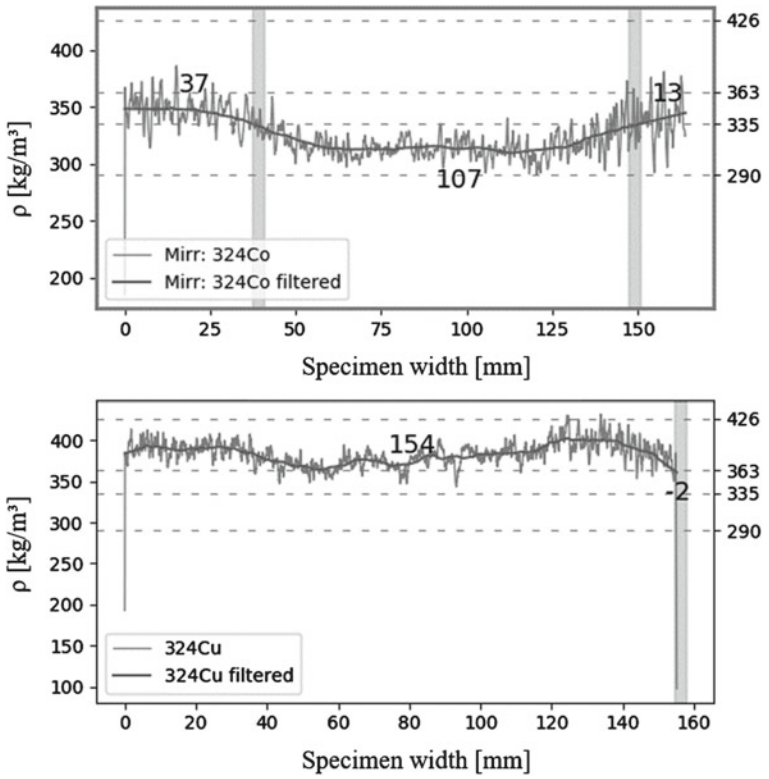

Fig. 3 Calculation of cutting positions and strip width based on the radiometric measured density profile (with and without smoothing) of the specimen from the upper and lower board end of 3/2/4 C

2.5 Testing Methods

The mean density of the beams was determined according to DIN 52182 [16]. Modulus of rupture (MOR) and local and global modulus of elasticity (MOE) of the GLT were determined in a four-point bending test according to [18]. The dimensions of the beams were 50 mm in width, 102 mm in height and 2200 mm in length. Due to expected large deflections, the specimen length corresponds to 21.5 times the specimen height instead of 19 times the height as recommended by EN 408 [18] to prevent the beam from slipping off the supports. A 20 kN testing machine was used for the C10 and a 100 kN testing machine for the C14 beams. For measuring the local and global MOE of the C10 beams, three inductive displacement transducers were used (two of type WA50 and one of type WA100; Hottinger Baldwin Messtechnik (HBM), Germany). The displacement values were recorded via a measuring amplifier (type

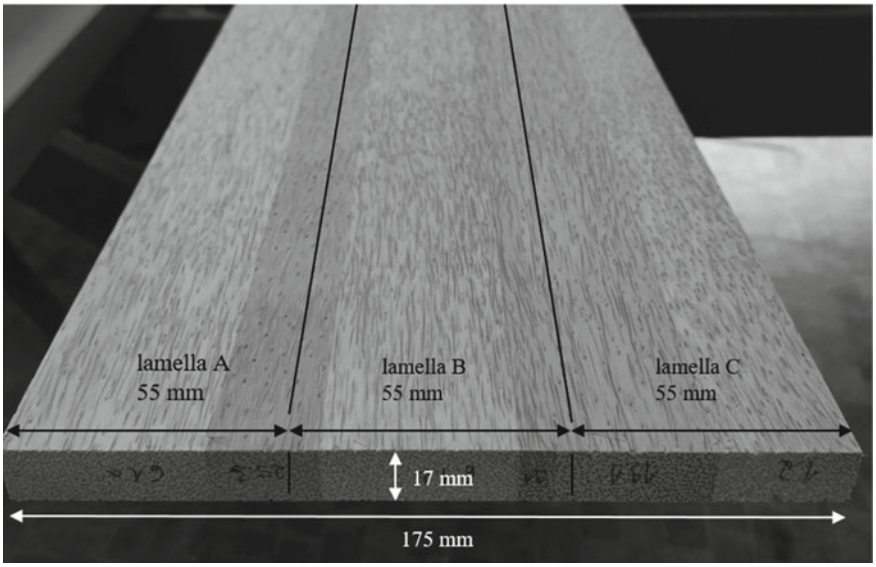

Fig. 4 Cross section of a calibrated edge-glued board for the production of ripped lamella based beams

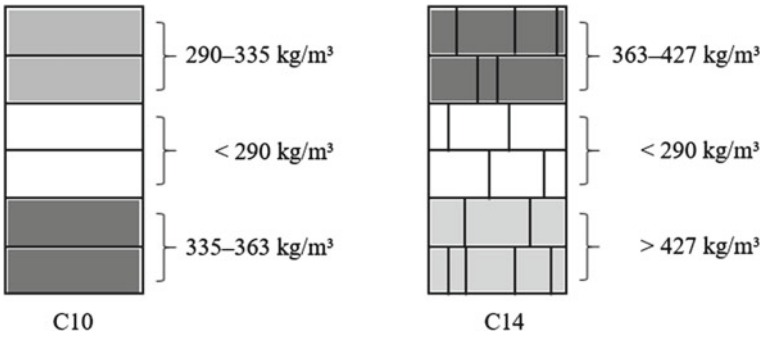

Fig. 5 Combined beam structures to achieve strength class C10 (left) and C14 (right). The left beam is based on non-ripped lamellas, whereas the beam on the right is based on ripped lamellas

HBM MX480A 4-channel measuring amplifier). The data as well as the control and calibration of the displacement transducers was recorded using the MX Assistant 4 software from HBM. The sampling rate of the displacement transducers was adapted to the sampling rate of the universal testing machine (100 Hz). The test speed was chosen so that any beam failure would occur within the time limit specified by EN 408 [18]. To determine the global MOE of the C14 beams a potentiometric displacement transducer was used (type 8712-10, burster Präzisionsmesstechnik, Germany). The local MOE was measured with the same inductive displacement transducers as used for the C10 beams (two of type WA50, HBM). The sensors were directly

Fig. 6 TimberPress X 300 (left) for pressing the GLT. Alignment of the GLT beams in the press, with lateral restraint between the beams (right)

connected to the computer of the testing machine, no measurement data amplifier was required. The test speed was controlled manually via a hydraulic unit. Plywood and oil palm wood supports of various dimensions were used to protect against support roller imprints when testing the C10 beams, plywood supports were used for the C14 beams. Deviating from EN 408 [18], the length of the supports (plywood) were three times the specimen width. The measuring range for determining MOE of the C10 beams was up to a force of 1200 N for both beam setups and for the C14 beams 600…1600 N for the non-ripped and 600…2400 N for the ripped beams.

Specimen geometry and test setup were corrected with k_h and k_l according to EN 384 [19]. The calculation of the characteristic values was done according to EN 14358 [20]. For the characteristic density (ρ_k) and strength ($f_{m,k}$) values, the parametric approach was taken due to the small number of test specimens and under the assumption of a normal distribution. Instead of the reduction factor k_s (n), which depends on the number of specimens, the value of the 5% quantile for a standard normal distribution ($p0.05 = 1.645$) was used in all calculations of the characteristic values in addition to the calculation according to the normalized reduction value for k_s (n).

3 Results and Discussion

3.1 Fracture Patterns and Failure Description

During the loading of the C10 beams on the 20 kN testing machine, unilateral longitudinal compression was observed in all beams either in front of or behind the supports and beneath the load inducing area. When the maximum longitudinal compressive strength was reached, the vascular bundles buckled, leading to compression failure (Fig. 7, left). However, this ductile compression failure did not lead to a drop in force, so the test load was increased further until the beams failed in tension on the outermost lamella. This tension failure usually occurred below the compressive failure. To prevent compression failure parallel to the vascular bundles, different support materials with various lengths were used.

Because of the observed compression failure next to the supports at the C10 beams, the C14 beams were tested with the same load beam, but on a larger (100 kN) testing machine. To avoid buckling of the vascular bundles and subsequent failure in compression, five beams (two non-ripped and three ripped) were tested under reverse loading (upside down). Lamellas with the highest density were on the top (on the compression side) of the beam, because according to Fruehwald-Koenig and Heister [11] the compression strength parallel to the vascular bundles correlates positively to the density. One reverse tested beam (non-ripped) failed in shear, one (ripped) in compression and three in tension (Fig. 7, right).

Fig. 7 Typical fracture patterns; left: in compression below the load inducing area and in the area of the supports; right: in tension on a reverse loaded beam

Table 1 Density values of the C10 and C14 beams

Strength class	Beam setup	$\rho_{\bar{x}}$ (kg/m^3)	ρ_{σ} (kg/m^3)	cv (%)	$\rho_k{}^{0.05}$ (kg/m^3)	$\rho_k{}^{k(s)}$ (kg/m^3)	*n*
C10	Non-ripped	361	5	1	353	346	3
	Ripped	403	13	3	381	361	4
C14	Non-ripped	414	10	2	398	390	8
	Ripped	434	14	3	410	399	5

$\rho_k{}^{0.05}$ = reduction factor k(s) = p(0.05) = 1.645
$\rho_k{}^{k(s)}$ = reduction factor k(s) according to EN 14358 [20]

3.2 Density

The mean densities of the ripped beams of both strength classes are higher than that of the non-ripped beams (Table 1). The coefficient of variation is in a similar range and varies between 1 and 3%. The difference in the characteristic density ($\rho_k{}^{0.05}$) of ripped and non-ripped C14 beams is less than that of the C10 beams.

3.3 Bending Strength

Figure 8 shows the positive trend between density (ρ) and bending strength ($f_{m,0,rf}$) after taking into account the reduction factors k_h and k_l (Fig. 8 and Table 2). The bending strength of the ripped beams ($f_{m,0,rf,r}$) is higher than that of the non-ripped beams at the same density and ranges between 22…27 MPa for the ripped C14 and 17…24.5 MPa for the ripped C10 beams. At a density of 400 kg/m^3, the ripped C10 and C14 beams show almost the same bending strength of 22.5…24 MPa.

The characteristic bending strength ($f_{m,k}{}^{0.05}$) of the ripped C14 beams is 21 MPa and comparable to that of the ripped C10 beams with 20 MPa (Table 2). The difference between the characteristic bending strength of the non-ripped C10 (11 MPa) and C14 (16 MPa) beams is higher. The characteristic values $f_{m,k}{}^{k(s)}$ according to [20] are 2…3 MPa lower than the $f_{m,k}{}^{0.05}$ values. The coefficient of variation ranges between 9…13% for the C14 and 7…8% for the C10 beams.

3.4 Bending Stiffness

Figure 9 shows the local MOE ($E_{m,0,l}$) for the different beam setups and strength classes. The range of the local MOE ($E_{m,0,l}$) of C14, especially the ripped beams, is the highest for all setups and strength classes. The lower values of the C14 are similar to the higher values of C10.

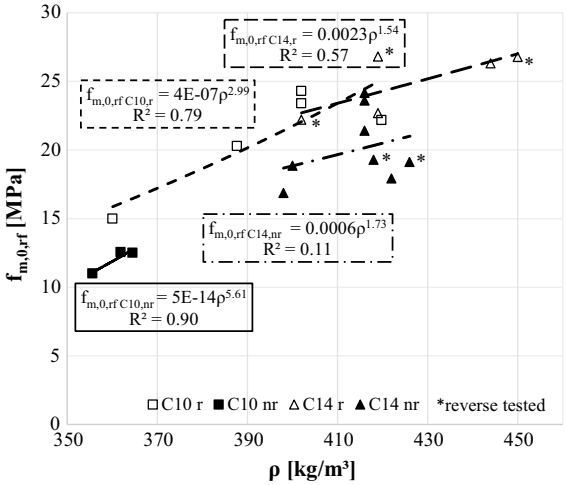

Fig. 8 Relationship between bending strength ($f_{m,0,rf}$) after considering the reduction factors k_h and k_l [19] (EN 384) and the GLT density

Table 2 Bending strength properties of GLT beams class C10 and C14

Strength class	Beam setup	$f_{m,\bar{x}}$ (MPa)	$f_{m,\sigma}$ (MPa)	cv (%)	$f_{m,k}^{0.05}$ (MPa)	$f_{m,k}^{k(s)}$ (MPa)	*n*
C10	Non-ripped	12	1	7	11	9	3
	Ripped	23	2	8	20	17	4
C14	Non-ripped	20	3	13	16	14	8
	Ripped	25	2	9	21	19	5

$f_{m,k}^{0.05}$ = reduction factor k(s) = p(0.05) = 1.645
$f_{m,k}^{k(s)}$ = reduction factor k(s) according to EN 14358 [20]

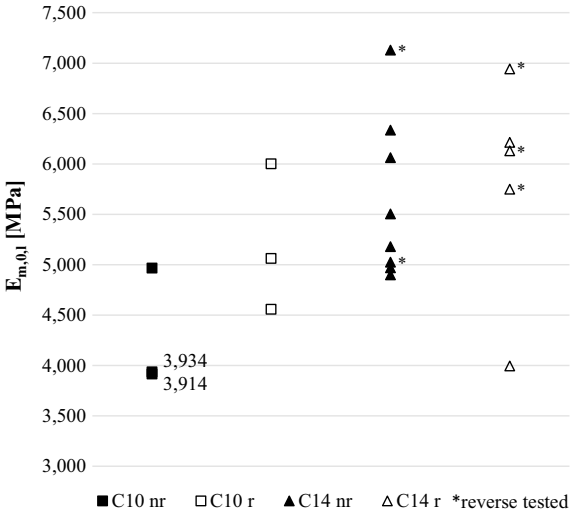

Fig. 9 Local MOE ($E_{m,0,l}$) of the different beam setups and strength classes

The statistical values for the local MOE are shown in Table 3. The ripped beams show a higher mean local MOE ($E_{m,0,l,\bar{x}}$) than the non-ripped beams and the C14 are higher than the C10. $E_{m,0,mean,l}{}^{0.05}$ of the non-ripped C14 beams is higher (4319 MPa) than that of the ripped C14 beams (3993 MPa) (due to one very low MOE value in the C14r, cf. Fig. 9). In contrast, $E_{m,0,mean,l}{}^{0.05}$ of the ripped C10 beams is higher (4000 MPa) than that of the non-ripped C10 beams (3283 MPa). $E_{m,0,mean,l}{}^{0.05}$ for ripped beams of both strength classes is almost similar (3993 MPa for C14 and 4000 MPa for C10). The coefficient of variation is 14%, except for the ripped C14 beams (cv = 19%).

The relationship between local MOE ($E_{m,0,l}$) and MOR ($f_{m,0,rf}$) of beams for different beam setups and strength classes is shown in Fig. 10. A positive trend between stiffness and strength is observed over the entire specimen range. Furthermore, the MOR ($f_{m,0,rf}$) of the ripped beams is higher for both strength classes than of the non-ripped beams. The strength of the ripped C14 beams is in the range of 22…27 MPa at a local MOE of 4000…7000 MPa.

Figure 11 shows the relationship between the local MOE ($E_{m,0,l}$) and global MOE ($E_{m,0,g}$) for oil palm wood beams with different setups and strength classes and the linear relationship for coniferous wood species according to EN 384 [19]. For all specimens, the local MOE ($E_{m,0,l}$) is above the global MOE ($E_{m,0,g}$), which is in accordance with most softwoods. All oil palm wood beams tested showed a positive linear correlation between the global and local MOE. But the linear relationship for softwoods according to EN 384 [19] does not apply to oil palm wood.

4 Conclusion

Density respectively the elastomechanical properties of the lamellas and lamella density-pre-grading and ripping influence the bending properties of GLT made of oil palm wood. Ripping boards according to their density into stripes and edge-gluing the stripes to density homogeneous lamellas results in higher MOR and MOE values for the GLT (due to the positive correlation between density and elastomechanical properties). Even the $f_{m,k}$ for non-ripped C14 beams ($f_{m,k} = 14$ MPa) is lower than for ripped C10 beams ($f_{m,k} = 17$ MPa). Designing beams with lamellas placed according to their density was shown to have a significant influence on the elastomechanical properties and fracture pattern of the beams. The local MOE of these beams is higher than the global MOE. The linear regression function between the local and global MOE for coniferous timber according to EN 384 [19] does not apply to beams made from oil palm wood. Due to the low number of specimens and limited variation in lamella densities, it cannot clearly be determined whether the local MOE values of ripped beams are higher than of non-ripped beams.

Table 4 shows the comparison of the characteristic values of strength classes C14–C22 for coniferous timber according to EN 338 [13] and the determined characteristic values for ripped and non-ripped C10 and C14 beams made of oil palm wood. The oil palm wood GLT C10 and C14 achieves the target MOR ($f_{m,k}$). Applying the reduction

Table 3 Local MOE properties of GLT beams class C10 and C14

Strength class	Beam setup	$E_{m,0,l,\bar{x}}$ (MPa)	$E_{m,0,l,\sigma}$ (MPa)	cv (%)	$E_{m,0,mean,l}^{0.05}$ (MPa)	$E_{m,0,mean,l}^{k(s)}$ (MPa)	N
C10	Non-ripped	4271	601	14	3283	3988	3
	Ripped	5205	733	14	4000	4860	4
C14	Non-ripped	5636	801	14	4319	5371	8
	Ripped	5804	1101	19	3993	5440	5

$E_{m,0,mean,l}^{0.05}$ = reduction factor k(s) = p(0.05) = 1.645
$E_{m,0,mean,l}^{k(s)}$ = reduction factor k(s) according to EN 14358 [20]

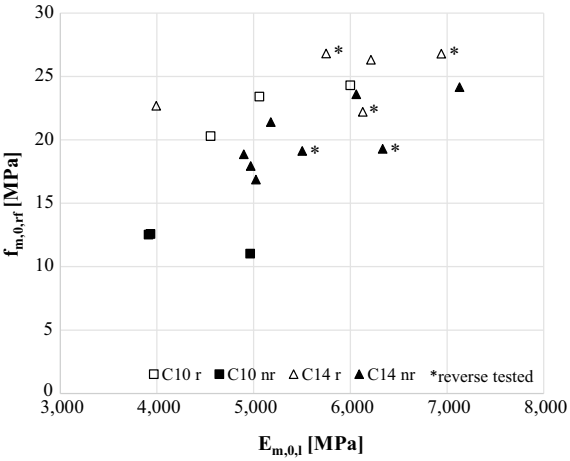

Fig. 10 Relationship between local MOE ($E_{m,0,l}$) and bending strength ($f_{m,0,rf}$) (after considering the factors k_h and k_l [19] (EN 384))

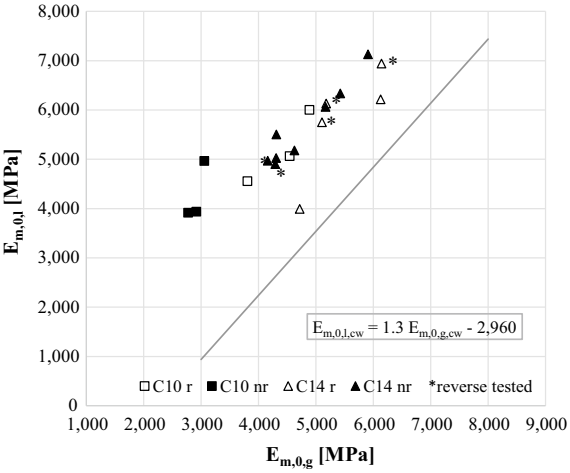

Fig. 11 Relationship between global MOE ($E_{m,0,g}$) and local MOE ($E_{m,0,l}$) for oil palm wood GLT and coniferous wood

factor for coniferous wood according to EN 14358 [20], the target $f_{m,k}$ is not fulfilled by the non-ripped C10 beams. Therefore, the calculated density limits for achieving a target characteristic strength and the calculation method are reasonable in principle. The target MOE for C14 according to EN 338 [13] ($E_{m,0,mean} = 7000$ MPa) is far from achieved. In contrast, the target density ($\rho_k = 290$ kg/m^3) of C14 according to EN 338 [13] is achieved by all oil palm wood beams.

The specific characteristic bending strength ($f_{m,k}/\rho_k$) of the oil palm wood GLT is between 26.0 and 47.6 MPa (Mg m^{-3})$^{-1}$, the ripped CLT are 47.1 (C10) and 47.6 (C14) MPa (Mg m^{-3})$^{-1}$. Therefore, the ripped are in the range of coniferous C14 (48.3 MPa (Mg m^{-3})$^{-1}$). In contrast, the specific mean MOE ($E_{m,0,mean}/\rho_{\bar{x}}$) of oil palm wood GLT is between 11.0 and 13.0 GPa (Mg m^{-3})$^{-1}$ and therefore much lower than that of coniferous C14 (20.0 GPa (Mg m^{-3})$^{-1}$). It can be concluded

Table 4 Characteristic values for strength, stiffness and density of oil palm GLT beams with grade C10[a] and C14[a] and for coniferous timber [13]. The characteristic values for oil palm beams are calculated according to EN 14358 [20]

	Oil palm timber				Coniferous timber				
Strength class	C10[a]		C14[a]		C14	C16	C18	C20	C22
	N-R	R	N-R	R					
$f_{m,k}$ (MPa)	9	17	14	19	14	16	18	20	22
$E_{m,0,mean}$ (MPa)	3988	4860	5371	5440	7000	8000	9000	9500	10000
ρ_k (kg/m^3)	346	361	390	399	290	310	320	330	340
$\rho_{\bar{x}}$ (kg/m^3)	361	403	414	434	350	370	380	400	410

[a]Defined grading classes for oil palm GLT beams according to strength classes for coniferous timber according to EN 338 [13]

that the relationship between the characteristic values for strength and density of coniferous timber according to EN 338 [13] fits for GLT from oil palm, but not the relationship between the mean MOE and density. The MOE is – in relation to strength and density – much lower for oil palm wood.

Acknowledgements The project was funded by the German Federal Ministry of Education and Research through the "Bioökonomie International 2017" project "Oilpalmsugar (031B0767A)". Leitz GmbH & Co. KG provided wood processing tools, Electronic Wood Systems the X-ray measurement device, Jowat SE the adhesives and MINDA Industrieanlagen GmbH the press.

Author Contributions Katja Fruehwald-Koenig is credited for the initial idea of ripping oil palm boards according to their density and the research questions, project goal and research approach. She also developed the oil palm wood strength classes and calculated their density limits. Lena Heister performed all laboratory tests, their analyses, and drew the figures and tables under the supervision of Katja Fruehwald-Koenig. Both authors wrote this paper together.

References

1. Fruehwald A, Fruehwald-Koenig K (2019) The use of oil palm trunks for wood products. In: Materials research proceedings of the 1st world conference on by-products of palm trees and their applications (ByPalma), 15–17 December 2018, Aswan, Egypt, p 11
2. Jumaat MZ, Rahim AHA, Othman J, Midon MS (2006) Strength evaluation of oil palm stem trussed rafters. Constr Build Mater 20(9):812–818
3. Srivaro S, Matan N, Lam F (2019) Performance of cross laminated timber made of oil palm trunk waste for building construction: a pilot study. Eur J Wood Wood Prod 77(3):353–365
4. Killmann W, Lim SC (1985) Anatomy and properties of oil palm stem. In: Proceedings national symposium of oil palm by-products, Kuala Lumpur, Malaysia
5. Lim SC, Gan K (2005) Characteristics and utilization of oil palm stem. Timber Bulletin: Forest Research Institut Malaysia, pp 1–7
6. Balfas J (2006) New approach to oil palm wood utilization for woodworking production part 1: basic properties. Indonesian J Forest Res 3(1):55–65

7. Erwinsyah SH (2008) Improvement of oil palm wood properties using bioresin. Dissertation, Technische Universität Dresden, Institut für Forstnutzung und Forsttechnik, Fakultät für Forst-, Geo- und Hydrowissenschaften, Dresden, 171p
8. Fathi L (2014) Structural and mechanical properties of the wood from coconut palms, oil palms and date palms. Dissertation, University of Hamburg, Zentrum Holzwirtschaft, Hamburg, 159p
9. Srivaro S, Matan N, Lam F (2018) Property gradients in oil palm trunk (Elaeis guineensis). J Wood Sci 64(6):709–719
10. Fruehwald-Koenig K (2019) Mechanical properties of oil palm wood. In: Presentation + Abstract on the CompWood2019, international conference on computational methods in wood mechanics—from material properties to timber structures ECCOMAS thematic conference, 17 June 2019, Växjö, Schweden
11. Fruehwald-Koenig K, Heister L (2022) Macromechanical and micromechanical behavior of oil palm wood (*Elaeis guineensis* JACQ.)—Part 1: tensile, compression and bending properties. Publication in preparation
12. Fruehwald-Koenig K (2019) Properties and grading of oil palm lumber. In: Wang X, Sauter U, Ross RJ (eds) 21th international nondestructive testing and evaluation of wood symposium; Freiburg, Germany, 24–27 September 2019, U.S. Department of Agriculture, Forest Service, Forest Products Laboratory, Madison, WI, pp 204–212
13. EN 338. Structural timber—Strength classes. Beuth Verlag, Berlin, 13p
14. EN 14081-2 (2018) Timber structures—strength graded structural timber with rectangular cross section—Part 2: machine grading; additional requirements for type testing. Beuth Verlag, Berlin, 39p
15. Koelli N (2016) Density and moisture distribution in oil palm trunks from Peninsular Malaysia. B.Sc thesis, University of Hamburg, Zentrum Holzwirtschaft, Hamburg, 52p
16. DIN 52182 (1976) Testing of wood; determination of density. Beuth Verlag, Berlin, 3p
17. DIN 50014 (2018) Standard atmospheres for conditioning and/or testing—specifications. Beuth Verlag, Berlin, 7p
18. EN 408 (2012) Timber structures—structural timber and glued laminated timber—determination of some physical and mechanical properties. Beuth Verlag, Berlin, 39p
19. EN 384. Structural timber—determination of characteristic values of mechanical properties and density. Beuth Verlag, Berlin, 21p
20. EN 14358. Timber structures—calculation and verification of characteristic values. Beuth Verlag, Berlin, 17p